

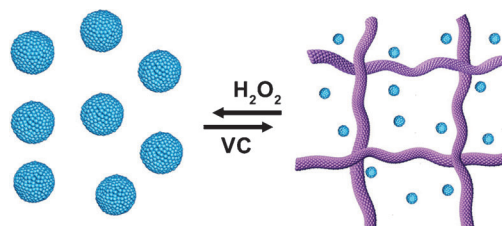
Communications



Self-Assembly

X. Miao, W. Cao, W. Zheng, J. Wang,
X. Zhang, J. Gao, C. Yang, D. Kong,*
H. Xu,* L. Wang,
Z. Yang* ————— ■■■-■■■

Switchable Catalytic Activity: Selenium-Containing Peptides with Redox-Controllable Self-Assembly Properties



Mimicking nature: The reversible formation of self-assembled nanostructures of selenium-containing peptides can be controlled by redox triggers (see scheme, VC = vitamin C). As a consequence, the

catalytic activity of these peptides is switchable. These results should lead to the development of nature-mimicking smart materials with promising properties.

Switchable Catalytic Activity: Selenium-Containing Peptides with Redox-Controllable Self-Assembly Properties**

Xiaoming Miao, Wei Cao, Wenting Zheng, Jingyu Wang, Xiaoli Zhang, Jie Gao, Chengbiao Yang, Deling Kong,* Huaping Xu,* Ling Wang, and Zhimou Yang*

Self-assembly is abundant in nature, ranging from relatively simple systems, such as lipid bilayers in cell membranes and the double-helical DNA structure, to the complex structures of organs. Many of these natural assemblies are dynamic and their formation is reversible, and extensive research efforts were recently made to develop smart materials by mimicking these dynamic self-assembly systems and their reversible formation.^[1,2] For instance, Van Esch and co-workers developed a dissipative-gel system by using a chemical fuel.^[3] The phosphatase/kinase switch widely used in biological systems to regulate protein activity and protein–protein interactions has also been applied to control the self-assembly of block polymers, polymer–polypeptide hybrids, and peptides.^[4] In order to form reversible-self-assembly systems, external stimuli are needed, which are usually the pH value, temperature, sonication, light irradiation, and additives.^[5,6] Among these stimuli, light irradiation is probably the most reliable and biocompatible one. Reversible self-assembly systems based on photoisomerizations have been widely studied and reported, including those of low-molecular-weight molecules and polymers.^[7,8] However, most of these methods cannot be applied *in vivo*, as our bodies have to maintain a relatively steady physical environment to function. Developing alternative and complementary strategies that are capable of reversibly switching bioactivity *in vivo* is in high demand.

Redox systems (e.g., NADH/NAD) have been widely used to regulate various biological activities, the disassembly of polymer micelles and nanogels, and the release of bioactive molecules.^[9] Inspired by these examples, we developed the molecular-hydrogel system of selenium-containing peptides with redox-controllable and reversible self-assembly and catalytic activity. Recently, the groups of Xu and Zhang developed a series of selenide- or diselenide-containing polymers with redox-controllable self-assembly properties.^[10] The reversible transformation between selenide and selenoxide was triggered by the addition of vitamin C (VC) and H₂O₂ (0.1 wt %). Vitamin C is biocompatible and the small difference in the chemical structure of selenide and selenoxide leads to huge differences in solubility and self-assembly properties of the polymers. Therefore, these systems have shown promising potential for controlled drug delivery and the generation of nature-mimicking systems. Stimulated by the achievements in redox-controllable self-assembly systems^[1,6,8] and self-assembly peptide systems,^[11] we opted to develop selenium-containing peptide systems with redox-controllable self-assembly propensity. Specifically, we intended to show that such redox control can regulate the catalytic activity of histidine-containing peptides by grafting the histidine to the selenium-containing peptides with different self-assembled nanostructures. We also planned to develop a biocompatible method for molecular hydrogelation by using VC to convert peptides that contain selenoxide to their reduced forms of selenide. In order to achieve these goals, we first designed compound **1** (Figure 1) containing the selenoxide group that could be reduced to selenide by VC, leading to the formation of compound **2**, which is less soluble in aqueous solutions. With the assistance of Phe-Phe (FF), compounds **1** and **2** might self-assemble into different kinds of nanostructures.

The synthetic route for compounds **1** and **2** is shown in Scheme S1 in the Supporting Information. First, 4-(phenylselenanyl)butanoic acid was synthesized in two steps in solution with a total yield of 41 %. It was then used in solid-phase peptide synthesis (SPPS) to obtain compound **2**. Pure compound **2**, which was obtained by high-performance liquid chromatography (HPLC), was oxidized with H₂O₂ (30 wt %, 2 equiv with regard to compound **2**) to produce compound **1**. This product could be solubilized in phosphate-buffered saline (PBS, pH 6.0) at concentrations lower than 3.0 wt % (30 mg mL⁻¹). A solution of compound **1** (1.0 wt %) in PBS could be converted to a hydrogel upon the addition of VC (1 equiv, final concentration of VC = 0.18 wt %; Figure 1). The minimum concentration for gelation of compound **1** was 0.45 wt % when it was treated with 1 equivalent of VC.

[*] X. Miao, Dr. L. Wang, Prof. Z. Yang
State Key Laboratory of Medicinal Chemical Biology and
College of Pharmacy, Nankai University
Tianjin 300071 (P. R. China)
E-mail: yangzm@nankai.edu.cn
Homepage: <http://yang-lab.org>

W. Cao, Prof. H. Xu
Key Lab of Organic Optoelectronics and Molecular Engineering
Department of Chemistry, Tsinghua University
Beijing 100084 (P. R. China)
E-mail: xuhuaping@tsinghua.edu.cn

W. Zheng, J. Wang, X. Zhang, J. Gao, C. Yang, Prof. D. Kong,
Prof. Z. Yang
State Key Laboratory of Medicinal Chemical Biology and
College of Life Sciences, Nankai University
Tianjin 300071 (P. R. China)
E-mail: kongdeling@nankai.edu.cn

[**] The authors acknowledge Prof. Yang Liu (Tsinghua University) for his kind discussion on electrochemistry measurements. This work was supported by the NSFC (51222303, 21074066, and 51003049) and the National Basic Research Program of China (2013CB834502).

Supporting information for this article is available on the WWW under <http://dx.doi.org/10.1002/anie.201303199>.

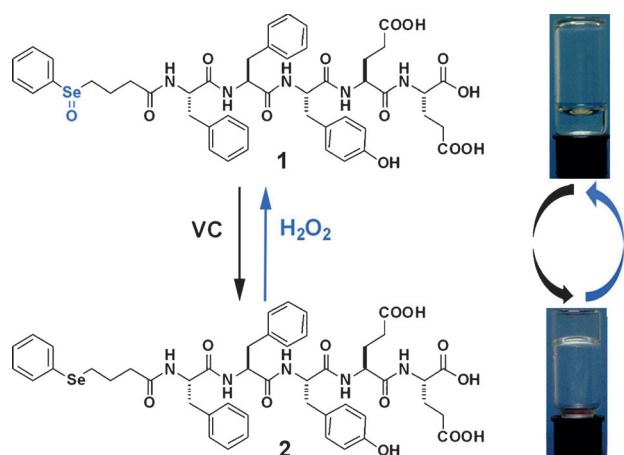


Figure 1. Chemical structures of selenium-containing peptides and optical images of a solution of **1** in PBS (1.0 wt%, pH 6.0) and a gel formed by treating the solution of **1** with vitamin C (1 equiv; the reversible transformation between **1** and **2** can be controlled by using vitamin C and H₂O₂).

The conversion from compound **1** to compound **2** and the mechanical properties of the hydrogel were analyzed by LC-MS and rheology, respectively. The LC-MS results (Figure S14) indicated that **1** was gradually converted to **2** by 1 equivalent of VC in PBS at 37°C. The conversion reached an equilibrium after about 7 hours with a conversion of about 65%. For the solution containing 1.0 wt% of **1** and 1 equivalent of VC, it took about 6 hours to form a hydrogel, and the conversion was about 59% at the gelling point. The minimum VC concentration to trigger the formation of a hydrogel from a solution containing 1.0 wt% of **1** was about 0.05 wt% (0.28 equiv with regard to **1**). An increase in the concentrations of VC or **1** resulted in shorter gelation times (Table S1). The resulting hydrogel could be converted back to a solution by the addition of H₂O₂ (Figure 1, and Figure S20 in the Supporting Information). This sol-gel-sol cycle could be repeated for at least three times without obvious decomposition of the compounds (LC-MS results of one cycle of transformation have been included in Figure S23).^[12] The dynamic frequency sweep (Figure S15) indicated that the hydrogel exhibited dependence on the frequency between 0.1 and 100 rad s⁻¹. The G'' value (viscosity) became closer to the G' value (elasticity) at higher frequencies. The G' values were lower than 100 Pa within the frequency range of 0.1–100 rad s⁻¹. These observations indicated the presence of a weak gel. Biocompatible triggers for the formation of hydrogels have recently attracted extensive research interests.^[13,14] The use of biocompatible VC to form hydrogels might advance the application of molecular hydrogels in tissue engineering and controlled drug release.

We then used transmission electron microscopy (TEM) to characterize the morphology of self-assembled structures in the solution and gel. Our observation of micelles with a size of 100–180 nm in the solution of compound **1** in PBS (Figure 2B) was consistent with the results obtained by dynamic light scattering (DLS, Figure S19). Upon the addition of 1 equivalent of VC, the micelles gradually changed to nanofibers with a diameter of about 30 nm (Figure 2C). These

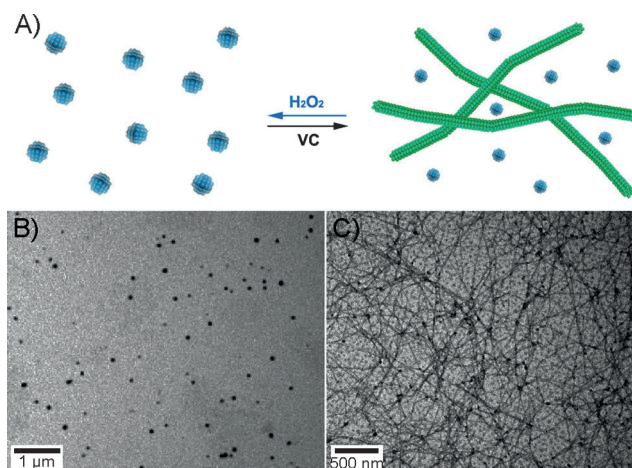


Figure 2. A) Illustration of the redox-triggered transformation between micelles and nanofibers; and TEM images of B) the solution of **1** in PBS (1.0 wt%) and C) the hydrogel resulting from the treatment of this solution with VC (1 equiv; image taken after 24 h treatment).

nanofibers, which were longer than 5 μm, entangled each other to form three dimensional (3D) networks for hydrogelation. We observed micelles between nanofibers in the gel because of the presence of about 35% of unconverted compound **1**. The size of the micelles in the gel decreased to about 25 nm. Upon the addition of H₂O₂ (0.1 wt%) to the gel, the nanofibers were converted back to micelles (Figure S24). These observations indicated that the propensity to self-assemble and the nature of the self-assembled structures of selenium-containing peptides could be controlled by the redox trigger. Circular dichroism (CD) spectra (Figure S17) indicated that compound **1** was present in a random-coil conformation and that peptides in the gel formed by VC adopted antiparallel β-sheet conformations.^[15] Many peptides with β-sheet conformations self-assemble into fibers and gels.^[13,16] However, we were unable to provide models to explain the formation of micelles and fibers. Based on the DLS results (Figure S18), the critical micelle concentration (CMC) was 2.5 and 2.2 mg mL⁻¹ for **1** and **2**, respectively. It was surprising that such a small difference in CMCs between the two compounds led to such a huge difference in the nature of the self-assembled nanostructures. Our system was similar to biological systems that use kinase/phosphatase to regulate their activity (a small difference in the chemical structure led to a big difference in the properties).^[17]

We also characterized compounds **1** and **2** by different techniques. The reverse-phase HPLC results showed that **1** and **2** had retention times of 3.4 and 4.5 min, respectively, thus indicating a change in the amphipathic property between the oxidized and reduced forms (Figure S12A). The results also indicated that the oxidized form (selenoxide) was more hydrophilic than the reduced form (selenide). The ESI-MS data (Figures S3 and S5) showed that the molecular ion peak shifted from 976.2874 ([M+H]⁺) to 960.2915 ([M+H]⁺) as a result of the reduction of **1** to **2**, thus demonstrating the existence of selenoxide and selenide structures. We also used ⁷⁷Se NMR spectroscopy to investigate the conversion between selenide and selenoxide. Compound **2**, which con-

tains selenide, showed a chemical shift of 285.71 ppm. After the oxidation by H_2O_2 , the chemical shift was 858.43 ppm, thus indicating the conversion from selenide to selenoxide (Figure S12B). We analyzed the change between the oxidized form (selenoxide) and the reduced form (selenide) by X-ray photoelectron spectroscopy (XPS). The binding energy of Se 3d⁵ of compound **2** was 55.2 eV (Figure S12C), which was similar to that of the selenide group. Compound **1** showed a binding energy of 55.7 eV. Selenoxide-containing compounds usually exhibited peaks around 57 eV.^[18] The lower binding energy of **1** was probably a result of the formation of hydrogen bonds between selenoxide and peptides, which might result in its disability to form supramolecular chains and fibers.

Since the propensity to self-assemble and the nature of the self-assembled nanostructures of selenium-containing peptides could be tuned by the redox trigger, we planned to place histidine-containing peptides on the surfaces of these nanostructures and to demonstrate the possibility to switch their hydrolysis activity. Our design and synthesis of compound **3** were comparable to that of **1** (Figure S25). Compound **3** bears a histidine residue, which is the active site of esterase enzymes. The reversible transformation between **3** and **4** could be achieved by redox control. This transformation leads to a different density of histidine residues on the surface of different kinds of nanostructures, resulting in the change in hydrolysis activity.

Similar to the reversible conversion between compounds **1** and **2**, the solution of compound **3** and gel of compounds **3** and **4** could also be switched by redox control (Figure 3 A and B, HEPES buffer, pH 7.4). We also observed the reversible transformation between the micelles in solution and the nanofibers in the gel (Figure 3 A and B). Since 97.3% of **3** was converted to **4**, we did not observe micelles in the TEM image of the gel after 24 hours. The higher conversion of **3** compared with that of **1** suggested that the sequence of the peptide or the morphology of the self-assembled structure might affect the equilibrium. The redox process of compound **4** was further investigated by cyclic voltammetry. Figure S31 B showed a reversible peak at 0.248 V and 0.188 V, corresponding to the redox couple **3/4**. The 60 mV difference between the two peaks suggested a two-electron transfer between selenide and selenoxide. Compared to the NADH/NAD transformation in biological systems, which exhibited an oxidation peak at 0.600 V (Figure S31 A), the reversible transformation between compounds **4** and **3** was more readily achieved. The control peptide (AcFFYEGH) showed no redox peak (Figure S31 C).

The $K_{\text{cat}}/K_{\text{M}}$ values of the peptide for the hydrolysis of acetal-4-nitrophenol to 4-nitrophenol were 10.5 and 1.1 for the solution (micelles) and the gel (fibers), respectively (Figure S30). The big difference in hydrolysis activity between solution and gel suggested that the catalytic activity could be switched by the redox trigger. The very slow increase in absorption intensity during the first five minutes (Figure 3C) indicated a slow rate of conversion from acetal-4-nitrophenol to 4-nitrophenol and a low catalytic activity of the nanofibers in the gel (97.3% of compound **3** in the gel). Upon the addition of H_2O_2 (0.1 wt%, 10 equiv), the nanofibers would

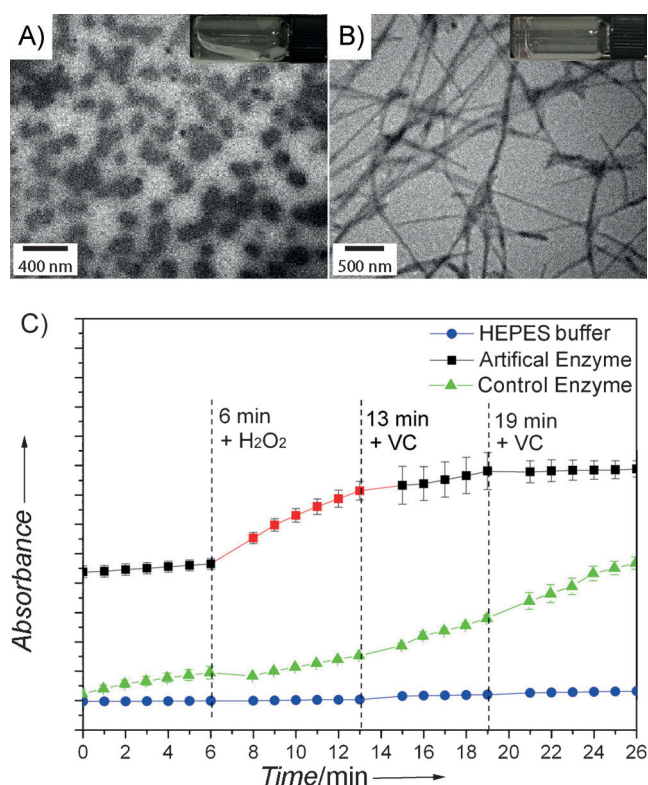


Figure 3. TEM images of A) a solution of **3** in HEPES buffer, and B) the gel resulting from treatment of this solution with VC (1 equiv; image taken after 24 h treatment (the inserts show the solution and gel, respectively). C) Absorbance (at 405 nm) upon the addition of H_2O_2 (10 equiv) and VC (20 equiv after 13 min and another 20 equiv after 19 min, control enzyme: peptide of Ac-YEGH). The absorbance increase indicated the conversion from acetal-4-nitrophenol to 4-nitrophenol mediated by the catalyst. The changes in absorbance indicated different catalytic activities. The assay was conducted in a two-phase system with acetal-4-nitrophenol in dichloromethane and the peptides in HEPES buffer, because the addition of high concentrations of H_2O_2 and VC to the aqueous solution of acetal-4-nitrophenol would have resulted in absorbance increases. HEPES = 2-[4-(2-hydroxyethyl)-1-piperazinyl]ethanesulfonic acid.

be partially converted to micelles (89.2% of compound **3** after 13 min), leading to a rapid increase in absorption intensity and a much higher catalytic activity (6–13 min in Figure 3C). The higher catalytic activity of the micelles compared with that of the fibers was probably due to the larger number of histidine residues at the surface of the micelles and their higher surface areas and mobility compared with those of fibers (Compounds **3** and **4** were about 3.5 nm long. Therefore, most of the histidine residues were buried in the inner part of the nanofibers, which have a diameter of about 50 nm and are longer than 5 μm , and micelles with a size of about 80–150 nm). The hydrolysis activity could also be decreased by the addition of VC (20 equiv after 13 min and another 20 equiv after 19 min; Figure 3C, 13–25 min). The rate, in which the activity decreased when VC was added was smaller than the rate, in which the activity increased, when H_2O_2 was added, because the conversion induced by VC is slower than that induced by H_2O_2 (94.5% and 97.1% of compound **3** after 19 and 25 min, respectively). Acetal-4-nitrophenol was not

- [15] N. J. Greenfield, *Nat. Protoc.* **2007**, *1*, 2876–2890.
- [16] A. R. Hirst, S. Roy, M. Arora, A. K. Das, N. Hodson, P. Murray, S. Marshall, N. Javid, J. Sefcik, J. Boekhoven, J. H. van Esch, S. Santabarbara, N. T. Hunt, R. V. Ulijn, *Nat. Chem.* **2010**, *2*, 1089–1094.
- [17] S. L. Porter, M. A. Roberts, C. S. Manning, J. P. Armitage, *Proc. Natl. Acad. Sci. USA* **2008**, *105*, 18531–18536; Y. Wang, F. Yang, Y. Fu, X. Huang, W. Wang, X. Jiang, M. A. Gritsenko, R. Zhao, M. E. Monore, O. C. Pertz, S. O. Purvine, D. J. Orton, J. M. Jacobs, D. G. Camp 2nd, R. D. Smith, R. L. Klemke, *J. Biol. Chem.* **2011**, *286*, 18190–18201.
- [18] C. D. Wagner, W. M. Riggs, L. E. Davis, J. F. Moulder, G. E. Muilenberg, *Handbook of X-Ray Photoelectron Spectroscopy*, PerkinElmer Corporation, U.S.A., **1979**.
- [19] S. Soukasene, D. J. Toft, T. J. Moyer, H. Lu, H. K. Lee, S. M. Standley, V. L. Cryns, S. I. Stupp, *ACS Nano* **2011**, *5*, 9113–9121; A. G. Cheetham, P. Zhang, Y. A. Lin, L. L. Lock, H. Cui, *J. Am. Chem. Soc.* **2013**, *135*, 2907–2910.
- [20] M. O. Guler, S. I. Stupp, *J. Am. Chem. Soc.* **2007**, *129*, 12082–12083; D. Zaramella, P. Scrimin, L. J. Prins, *J. Am. Chem. Soc.* **2012**, *134*, 8396–8399; A. Barnard, D. K. Smith, *Angew. Chem.* **2012**, *124*, 6676–6685; *Angew. Chem. Int. Ed.* **2012**, *51*, 6572–6581.
-